

THERMAL LENS COMPENSATION IN HIGH AVERAGE POWER DIODE PUMPED Nd:YVO₄ LASER USING ASPHERIC MIRROR

D. Stučinskas^a A. Varanavičius^a R. Antipenkov^a M. Grishin^{b,c} J. Kodz^b
A. Melninkaitis^a, and A. Vanagas^a

^a *Department of Quantum Electronics, Vilnius University, Saulėtekio 9, LT-10222 Vilnius, Lithuania*
E-mail: darius.stucinskas@ff.vu.lt

^b *EKSPLA Ltd, Savanorių 231, LT-02300 Vilnius, Lithuania*

^c *Institute of Physics, Savanorių 231, LT-02300 Vilnius, Lithuania*

Received 18 July 2009; revised 18 December 2009; accepted 18 December 2009

We demonstrate a high-power, diode-pumped, pulsed Nd:YVO₄ laser with a 1.2 diffraction-limited output of 9.5 W using a thin film deposition technology made aspheric mirror to correct the thermally induced phase distortion of the lasing medium.

Keywords: Nd:YVO₄, thermal lens compensation, diode-pumped, aspheric optics

PACS: 42.55.Xi, 42.60.By

1. Introduction

High average power picosecond lasers have been studied intensely because of their suitability for industrial applications such as laser micromachining [1–3], drilling precise holes for fuel injection [4], thin film patterning for solar cells [5].

Neodymium doped yttrium vanadate (Nd:YVO₄) crystal is a promising material for high average power picosecond lasers, because of its large stimulated emission cross-section and broad emission band, in comparison with conventional Nd:YAG [6, 7]. However, the power scaling of Nd:YVO₄ lasers is limited by thermally induced optical distortions that are quite significant in these lasers due to poor thermal properties of active medium leading to severe degradation of beam quality. The spherical component of thermal lens can be compensated by proper laser cavity design, i. e. choosing right radius of curvature and position of spherical resonator's components. Nevertheless, the non-spherical component cannot be compensated in the same manner. This leads to reduced efficiency and multi-mode oscillation as the heat load increases. Spherical aberrations of thermal lens of the active media are quite severe when the solid state lasers are strongly pumped. The aberrations influence the diffraction loss, the output power, the mode profile, and other laser beam properties [8].

Diffraction limited output has been demonstrated in high average power fibre lasers [9]. However, this technology has limited applications in high peak power lasers due to limited aperture of amplifying media that causes optical damage problems and appearance of nonlinear effects at relatively low laser energies. In this case, traditional end-pumped rod laser still holds its importance due to technical simplicity and virtually unlimited clear aperture. However, the performance of bulk-crystal based high power lasers is always limited by a thermal loading which causes thermo-optical and thermomechanical perturbations. This is particularly important for longitudinally pumped systems where large thermal gradients arise from deposition of heat within a small volume near the pump facet of the laser crystal. Therefore, thermal lens mitigation is crucial for efficient diode end pumped laser design.

Effective thermal lens compensation in diode-pumped and flash-lamp lasers employing phase conjugation has been demonstrated [10, 11]. Due to added complexity, this approach, however, is not desirable for industrial application aimed laser design. Alternative technique for thermal lens aberration correction is the use of adaptive and deformable mirrors [12, 13]. However, mirrors based on MEMS or piezocrystals are relatively expensive and sometimes also lack in lateral resolution. Recently a thermo-optically driven adaptive mirror based on thermal expansion has been proposed

[14, 15]. Although adaptive mirrors would allow thermal lens compensation in a wide range of operation, the complexity introduced is not always justified. As a good alternative to the expensive adaptive mirror a suitably shaped optical element, designed to cancel thermal distortions can be used instead [16, 17].

In this paper, we present the results on compensation of thermal lens aberrations of high average power Nd:YVO₄ laser by the use of aspherically shaped optical element. The highly reflecting optical element was shaped basing on measurements of actual thermal lens aberrations in active element, and manufactured using thin film deposition technology.

2. The experimental set-up and measurements of thermal lens aberrations

Experimental laser set-up (Fig. 1) is based on optical layout of PL10100 (produced by Ekspla) regenerative amplifier. PL10100 features high pulse energy (up to 200 μJ), high beam quality ($M^2 < 1.5$), and a high repetition rate (up to 100 kHz) of typically less than 10 ps pulses. It consists of a diode-pumped passively mode-locked Nd:YVO₄ oscillator and a diode-pumped regenerative amplifier [18]. However, parameters of this laser are optimized for highest output power which results in high lasing threshold and reduced beam quality at lower pump powers. Correction of thermally induced phase distortion in regenerative amplifier's active element could further improve parameters of this laser system in various operation regimes.

In order to design appropriate optics for thermal lens compensation we have performed the measurements of thermally induced lens in active medium when laser is operated at highest available pump powers. Experimental laser layout for thermal lens measurements is shown in Fig. 1. Active element (AE) is a 14 mm long Nd:YVO₄ crystal of 0.3% Nd concentration with 3 mm undoped caps on both ends. Aperture size of AE is $3 \times 3 \text{ mm}^2$. AE is pumped from both sides by two fibre coupled laser diode modules.

We employed a Shack–Hartmann wavefront sensor for measurement of the phase distortions acquired by probe beam of He-Ne laser after passing the pumped laser crystal. The Shack–Hartmann wavefront sensor was built using 40×40 lenslet array with lenslet size of $108 \mu\text{m}$ and Dalsa 1M15 CCD camera. In order to match the dimensions of pumped region in laser crystal and lenslet array we used a magnifying $4f$ imaging lens system. Measured probe beam wavefront cross-section after passing the laser active element (at 26 W

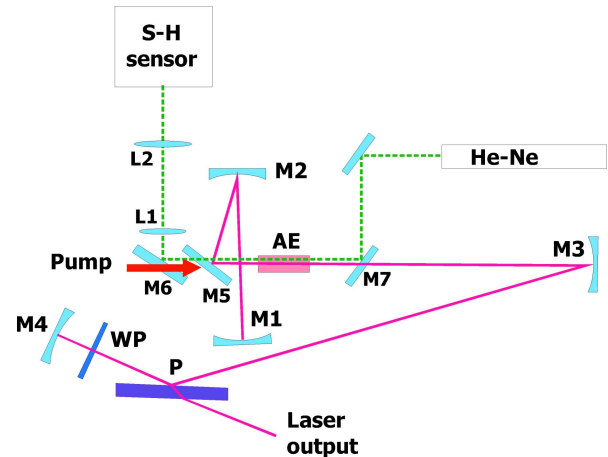


Fig. 1. Set-up for measuring the thermal lens focusing power in laser active element by means of Shack–Hartmann sensor. $M1$, $M2$, $M3$, and $M4$ are cavity mirrors (with their respective R equal to -1275 , 4000 , -340 , and -333 mm), P is polarizer, WP is a $\lambda/4$ phase plate, $M5$ is pump coupling mirror, $M6$ and $M7$ are HT@1064 HR@632 mirrors for Shack–Hartmann wavefront sensor probe beam. $L1$ and $L2$ are $4f$ imaging system lenses. Thermal lens aberration compensator was designed to replace the $M2$ cavity mirror.

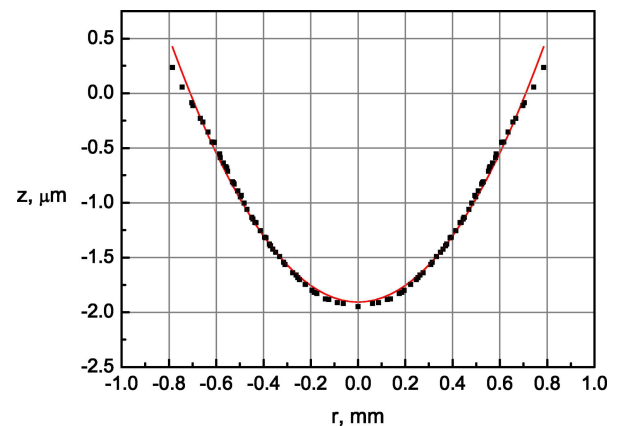


Fig. 2. Measured probe beam wavefront after passing the laser active element. Dotted line marks measured spots, continuous line is for $r = 230 \text{ mm}$ sphere (at 26.5 W pump power).

pump) is shown in Fig. 2. Thermal lens focal length ($f = 230 \text{ mm}$) was evaluated by fitting spherical wavefront to measured data. We have calculated thermal lens aberration by deducing spherical wavefront from measured data (see Fig. 3).

3. Design, production, and characterization of spherical wave compensators

The set of 10 samples for thermal lens compensation experiments were manufactured using thin film deposition technology. The same technique which is typically used for manufacturing of gradient filters is applied

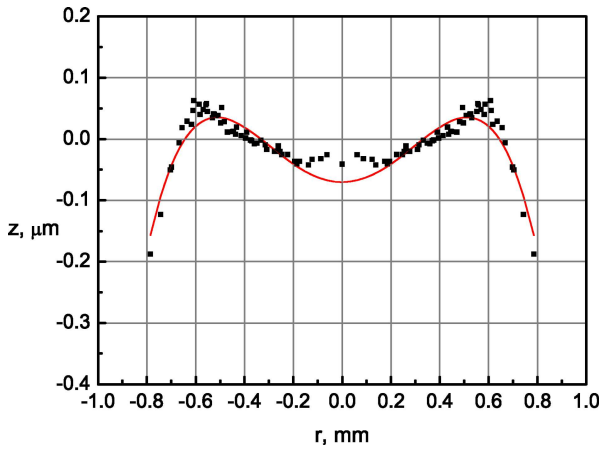


Fig. 3. Measured probe beam wavefront aberration after passing the laser active element. Dotted line marks measured spots, continuous line is a fitted spherical aberration.

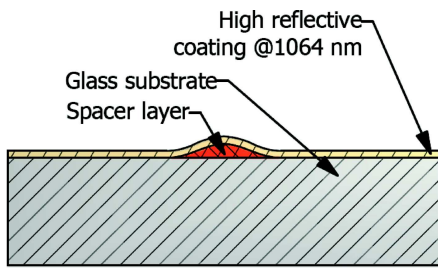


Fig. 4. Thermal lens aberration compensator design.

(Fig. 4). In order to form the profile of mirror surface that is required for compensation of thermal lens aberration, a Gaussian-shaped spacer layer was deposited through the appropriate aperture on the geometric centre position of each concave ($R = -1750$ mm) BK7 substrate. Every sample had different spacer layer parameters (width and height) that were designed in order to match the cavity mode parameters at compensator position in laser cavity and the thermal lens estimations obtained by Shack–Hartmann sensor. All substrates with spacer layer were further coated with high reflective (HR) conventional alternating $\lambda/4$ dielectric layers centred at $\lambda = 1064$ nm wavelength.

The wavefront distortions arising when probe beam is reflected from the curved compensator mirror surface were characterized using the so-called off-axis digital holography (DH) technique. DH imaging technique is capable of providing a phase-contrast image of three-dimensional surface structure of the specimen by computational means with a single hologram (interferogram) acquisition [19, 20].

Michelson interferometer and CCD sensor were used for digital hologram registration in CCD plane. The experimental scheme is equivalent to that described in [21].

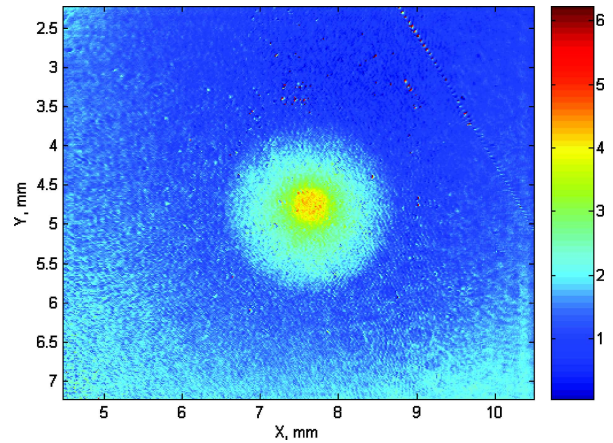


Fig. 5. Typical compensator phase difference diagram in reflected light obtained by digital holography.

As a coherent light source for DH measurements we use spatially filtered and collimated radiation of Q-switched and frequency tripled Nd:YAG laser, producing pulses of ~ 4 ns duration at the wavelength of 355 nm with 10 Hz repetition rate. In fact the use of 355 nm instead of 1064 nm increases the resolution of interferometric measurements. The distance of 165 mm between the testing HR mirror and surface of CCD sensor was set. The numerical algorithm was further employed to extract the phase information of reflected light [18]. The typical phase difference diagram in reflected light obtained by DH is shown in Fig. 5. Compensator can be seen as a curved mirror with aberration. From the phase information the relative surface height of thermal lens compensators can be extracted by using the relation

$$h = \frac{\Delta\varphi}{2\pi} \lambda.$$

Here $\lambda = 355$ nm is the wavelength used in DH measurements and $\Delta\varphi$ is the phase difference in the wavefront of reflected light. The height profile extracted from phase information is shown in Fig. 6.

From sample measurement results, we estimate that sample K010 profile exhibits best match to measured thermal lens aberration presented in Fig. 3.

4. Experimental results

Thermal lens aberration compensators were placed in place of $M2$ mirror (see Fig. 1). Kinematic $M2$ mirror mount was attached to XYZ stage, to provide necessary degrees of freedom for optimal placement of compensator. The main criteria for compensator positioning in resonator was TEM_{00} output beam profile, M^2 parameter, and output power. As compensator is

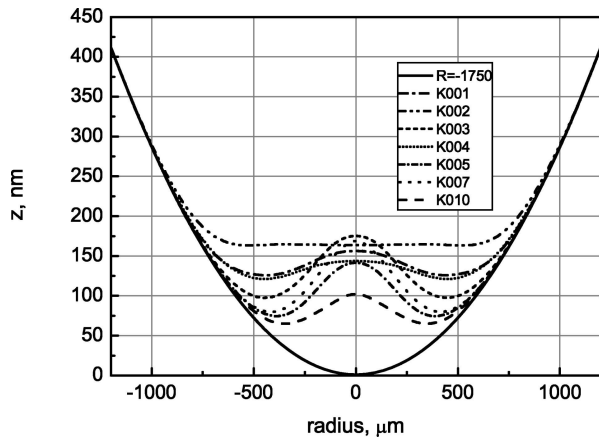


Fig. 6. Typical cross-section of measured thermal lens compensator.

manufactured on spherical substrate, it can be considered as aberration compensator plus spherical mirror. By deducing aberration from compensator profile, the radius of this spherical mirror was evaluated. We estimated that concave $R = -2000$ mm curvature radius mirror was a closest match for K010 compensator. Therefore, laser performance with $R = -2000$ mm mirror had to be investigated as well, in order to find out whether the laser performance changed because of different curvature mirror.

Initially, laser performance was investigated with a convex $R = 4000$ mm curvature radius $M2$ mirror that was a standard element in PL10100 cavity. Laser free-running output power, beam quality parameter M^2 , and output beam profile were measured. The same measurements were performed with 10 compensators. Measured laser output power dependence on pump power in continuous wave (CW) operation regime is shown in Fig. 7. The highest slope efficiency was ob-

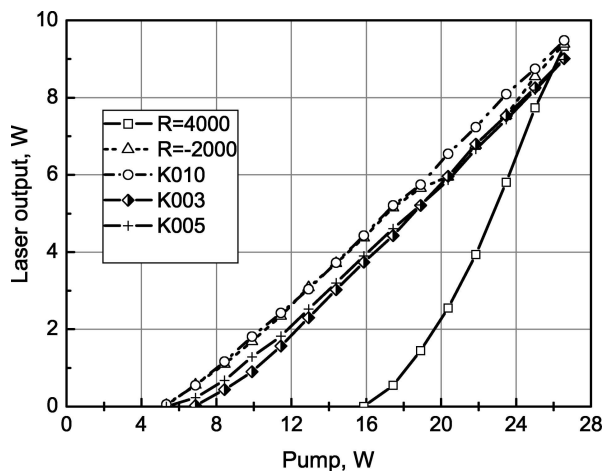


Fig. 7. Measured laser output power dependence on pump power in CW mode operation.

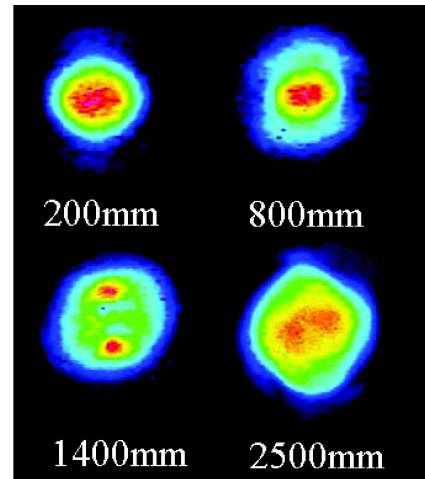


Fig. 8. Output beam intensity profile at various distances from output coupler when using $R = 4000$ mm curvature radius $M2$ mirror.

tained when using $R = 4000$ mm mirror. Maximum output power is closely the same for all samples tested. However, lasing threshold is almost 3 times smaller with compensator K010 and $R = -2000$ mm mirror as compared to the case with $R = 4000$ mm mirror.

Beam intensity profile was measured by CCD camera at 200–2500 mm distance from the laser output. These measurements were performed at maximum pump power, with different $M2$ mirrors and thermal lens compensators. In the case when $M2$ curvature is $R = 4000$ mm the output beam near field profile is nearly Gaussian (see Fig. 8). However, due to thermal lens aberrations, intensity distortions are clearly visible in 1–2 m distance. As aberration component diverges (at distances 2.5 m and above), output beam profile becomes Gaussian. By replacing $M2$ mirror with compensator, significant output beam quality improvement has been achieved (see Fig. 9). Laser output mode and power are sensitive to compensator X – Y position, but relatively insensitive to its Z position. Maximum laser output power with compensator can be higher by up to ~ 1.5 W (compared to performance with $R = 4000$ mm mirror), however, at the expense of beam quality.

Output beam quality was measured with Spiricon M2-200 Beam Propagation Analyzer. The results on beam quality parameter M^2 versus output power is presented in Fig. 10.

With mirror ($M2$) $R = 4000$ mm, ~ 9.5 W output power and beam quality parameter $M^2 = 1.2$ were achieved at highest pump powers. However, output beam profile at 1–2 m distance from output coupler was unsatisfactory. For industrial applications, where laser is operating at highest output powers, high threshold is not an issue, but when lower output powers are

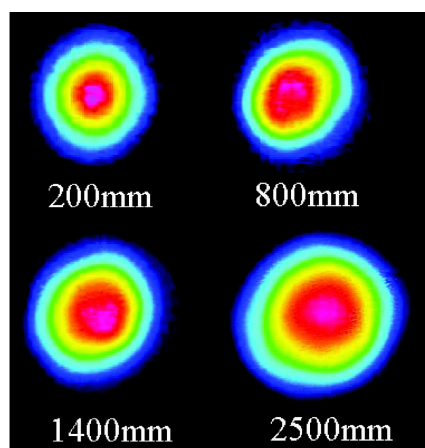


Fig. 9. Output beam intensity profile at various distances from output coupler when using K010 compensator.

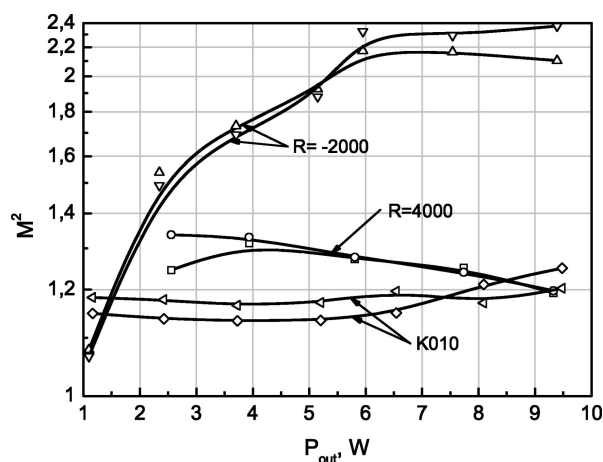


Fig. 10. Laser output beam M^2 parameter at different output powers (with different M^2 mirrors and K010 compensator).

needed, pump to output conversion efficiency drops rapidly. Replacing $R = 4000$ mm mirror by $R = -2000$ mm, lasing threshold was reduced by more than 3 times, however, without positive impact on output beam profile and resulted in worse output beam quality parameter M^2 (above 2 at highest pump powers). Aberration compensator, on the other hand, has improved all parameters mentioned above. Although output power has been increased only by few percent, threshold is more than 3 times lower and output beam quality parameter M^2 does not exceed 1.2 in wide pump power range. Moreover, output beam profile has significantly improved compared to results achieved with $R = 4000$ mm M^2 mirror.

5. Summary

The static aberration compensator approach was shown to be well suited for high-power diode pumped

lasers. This method has the advantages of greater simplicity and a wide applicability to laser designs. We have demonstrated a diode-pumped Nd:YVO₄ laser with a 1.2 diffraction-limited output of 9.5 W using a thin film deposition technology made aberration compensator to correct the thermally induced phase distortion of the lasing medium. Employment of proper thermal lens aberration compensator allowed for laser threshold reducing and ensured improved output beam quality parameter M^2 in wide pump power range.

Acknowledgement

This work was partially financed by the Lithuanian State Science and Studies Foundation under the project Nr. G-35/08.

References

- [1] D.M. Karnakis, M.R.H. Knowles, P.V. Petkov, T. Dobrev, and S.S. Dimov, Surface integrity optimisation in ps-laser milling of advanced engineering materials, in: *Proceedings of the 4th International WLT Conference on Lasers in Manufacturing*, Munich, Germany (2007).
- [2] C. Moorhouse, Industrial applications of a fiber-based high-average-power picosecond laser, *Proc. SPIE* **7201**, 72010F (Feb. 24, 2009).
- [3] http://www.ekspla.com/repository/catalogue/infosfiles/IL/application_notes/M1104_short_pulse_lasers_for_microfabrication.pdf.
- [4] M. Kraus, S. Collmer, S. Sommer, and F. Dausinger, Microdrilling in steel with frequency-doubled ultrashort pulsed laser radiation, in: *Proceedings of the 8th International Symposium on Laser Precision Microfabrication*, Vienna, Austria (2007).
- [5] S. Haas, A. Gordijn, and H. Stiebig, High speed laser processing for monolithical series connection of silicon thin-film modules, *Prog. Photovolt. Res. Appl.* **16**, 195–203 (2008).
- [6] A.W. Tucker, M. Birnbaum, C.L. Fincher, and J.W. Erler, Stimulated-emission cross section at 1064 and 1342 nm in Nd:YVO₄, *J. Appl. Phys.* **48**, 4907–4911 (1977).
- [7] D. Shen, A. Liu, J. Song, and K. Ueda, Efficient operation of an intracavity-doubled Nd:YVO₄ KTP laser end pumped by a high-brightness laser diode, *Appl. Opt.* **37**, 7785–7788 (1998).
- [8] C. Liu, T. Riesbeck, X. Wang, J. Ge, Z. Xiang, J. Chen, and H.J. Eichler, Influence of spherical aberrations on the performance of dynamically stable resonators, *Opt. Commun.* **281**, 5222–5228 (2008).
- [9] Y. Jeong, J. Nilsson, J.K. Sahu, D.N. Payne, R. Horley, L.M.B. Hickey, and P.W. Turner, Power scaling of

- single-frequency ytterbium-doped fiber master oscillator power amplifier sources up to 500 W, IEEE J. Sel. Topics Quantum Electron. **13**, 546–551 (2007).
- [10] D.A. Rockwell, A review of phase-conjugate solid-state lasers, IEEE J. Quantum Electron. **24**, 1124–1140 (1988).
- [11] Y. Ojima, K. Nawata, and T. Omatsu, Over 10-watt pico-second diffraction-limited output from a Nd:YVO₄ slab amplifier with a phase conjugate mirror, Opt. Express **13**, 8993–8998 (2005).
- [12] J. Schwarz, M. Ramsey, D. Headley, P. Rambo, I. Smith, and J. Porter, Thermal lens compensation by convex deformation of a flat mirror with variable annular force, Appl. Phys. B **82**, 275–281 (2006).
- [13] W. Lubeigt, G. Valentine, and D. Burns, Enhancement of laser performance using an intracavity deformable membrane mirror, Opt. Express **16**, 10943–10955 (2008).
- [14] F. Reinert and W. Lüthy, Thermo-optically driven adaptive mirror based on thermal expansion: preparation and resolution, Opt. Express **13**, 10749–10753 (2005).
- [15] F. Reinert, M. Gerber, W. Lüthy, and T. Graf, Laser resonator with a thermo-optically driven adaptive mirror, in: *Advanced Solid-State Photonics, Technical Digest* (Optical Society of America, 2005), WB27.
- [16] S.C. Tidwell, J.F. Seamans, and M.S. Bowers, Highly efficient 60-W TEM₀₀ cw diode-end-pumped Nd:YAG laser, Opt. Lett. **18**, 116–118 (1993).
- [17] J.J. Kasinski and R.L. Burnham, Near-diffraction-limited, high-energy, high-power, diode-pumped laser using thermal aberration correction with aspheric diamond-turned optics, Appl. Opt. **35**, 5949–5954 (1996).
- [18] EKSPLA, www.ekspla.com.
- [19] E. Cuche, P. Marquet, and C. Depeursinge, Simultaneous amplitude-contrast and quantitative phase-contrast microscopy by numerical reconstruction of Fresnel off-axis holograms, Appl. Opt. **38**, 6994–7001 (1999).
- [20] E. Cuche, P. Marquet, and C. Depeursinge, Spatial filtering for zero-order and twin-image elimination in digital off-axis holography, Appl. Opt. **39**, 4070–4075 (2000).
- [21] E. Cuche, F. Bevilacqua, and Ch. Depeursinge, Digital holography for quantitative phase-contrast imaging, Opt. Lett. **24**, 291–293 (1999).

ŠILUMINIO LĖŠIO KOMPENSAVIMAS ASFERINIŲ VEIDRODŽIŲ DIODINIO KAUPINIMO DIDELĖS VIDUTINĖS GALIOS Nd:YVO₄ LAZERYJE

D. Stučinskas^a, A. Varanavičius^a, R. Antipenkov^a, M. Grishin^{b,c}, J. Kodz^b, A. Melninkaitis^a, A. Vanagas^a

^a Vilniaus universitetas, Vilnius, Lietuva

^b UAB EKSPLA, Vilnius, Lietuva

^c Fizikos institutas, Vilnius, Lietuva

Santrauka

Pateikiami šiluminio lėšio sferinės aberacijos kompensavimo panaudojant asferinius rezonatoriaus elementus išilginio diodinio kaupinimo Nd:YVO₄ regeneratyviniame stiprintuve tyrimo rezultatai. Asferiniai optiniai elementai buvo pagaminti naudojant plynasluoksnių dangų garinimo technologiją. Šiluminio lėšio aberacijos buvo išmatuotos Shack'o ir Hartmann'o bangos fronto matuokliu. Remiantis matavimų rezultatais, pagaminta 10 kompensatorių, skirtų sferinės aberacijos korekcijai: ant sferinio BK7 pagrindėlio buvo užgarinti Gauso formos iškilumai. Vienas nuo kito kompen-

toriai skyrėsi skirtingu užgarinto iškilumo aukščiu bei pločiu. Optimali kompensatoriaus padėtis rezonatoriuje buvo nustatoma atsižvelgiant į lazerio išvadinę galią bei lazerio išvadinio pluošto kokybės parametą M^2 . Naudojant asferinį kompensatorių, generavimo slenkstis sumažėjo daugiau kaip 3 kartus, taip pat žymiai pagerėjo lazerio pluošto intensyvumo skirstinys. Matuojant pluošto kokybės parametrus nustatyta, kad naudojant kompensatorius M^2 yra mažesnis nei 1,2 visame lazerio veikimo diapazone, tuo tarpu be kompensatoriaus M^2 būna nuo 1,2 iki 1,4.